

Climate response over Asia/Arctic to change in orbital parameters for the last interglacial maximum

Seong-Joong Kim* *Korea Polar Research Institute (KOPRI), KORDI, PO Box 32, Incheon 406-840, Republic of Korea*
Jun Mei Lü *Chinese Academy of Meteorological Sciences, Beijing 100081, China*
Sangheon Yi *Korea Institute of Geoscience and Mineral Resources (KIGAM), Daejeon 305-350, Republic of Korea*
Taejin Choi
Baek-Min Kim
Bang Yong Lee
Sung-Ho Woo
Yoojin Kim

} *Korea Polar Research Institute (KOPRI), KORDI, PO Box 32, Incheon 406-840, Republic of Korea*

ABSTRACT: The climate response over Asia/Arctic to the change in orbital parameters for the last interglacial maximum (LIGM) is investigated using the NCAR CCM3. After implementing LIGM orbital parameters, the insolation decreases in January and increases in July in the northern hemisphere in comparison to present values. The reduced net short-wave radiative heat fluxes in January lead to the surface cooling in low to mid latitudes of Asia, whereas a warming is obtained in northern Asia where the net short-wave radiative heat fluxes change little. The January warming in northern Asia/Arctic in the LIGM, consistent with proxy records, is mainly due to the marked increase in downward long wave heat fluxes associated with the increase in cloud and in part by the increase in the Arctic Oscillation polarity. In July, the increased insolation leads to the surface warming over most Asia, even though a slight cooling is obtained in low latitudes in spite of the increase in insolation, due to the decrease in the short-wave heat fluxes at the surface by the increase in the cloud amount. Precipitation overall increases at South and East Asia in July, due to the stronger southwest and southerly winds. The change in insolation due to the orbital parameters determines the climate change pattern in low- to mid-latitudes over Asia in the LIGM, even though the degree of climate change is much lower than suggested by proxy estimates. The results obtained in this study implies that, under the different climate background such as future global warming, the change in greenhouse effect associated with cloud feedback could play an important role in determining the climate change over Asia/Arctic.

Key words: last interglacial maximum, climate change, numerical simulation, Asia/Arctic, orbital parameters

1. INTRODUCTION

The last interglacial maximum (LIGM) occurred at 126,000 years before present (BP) provides opportunity to investigate the effect of orbitally induced insolation changes on regional climates (Kukla et al., 2002; CAPE–Last Interglacial Project Members, 2006). Many of paleoclimate proxy

data have indicated that the LIGM climate was as warm as or warmer (from about 0.5 °C to 2.0 °C) than present (van der Hammen et al., 1971; Ruddiman and McKintyre, 1976; Woilard, 1978; Keen et al., 1981; Mangerud et al., 1981; Miller et al., 1983; De Vernal et al., 1986; LIGA members, 1991; Cortijo et al., 1994; Zagwijn, 1996; Aalbersberg and Litt, 1998; Kukla et al., 2002; EPICA Community members, 2006; CAPELast Interglacial Project Members, 2006, and references there in) and sea level was about 6 m higher than present level (Bloom et al., 1974; Ku et al., 1974; Dodge et al., 1983), due to the melting of the west Antarctic ice sheet (Stuiver et al., 1981) and melting of the Greenland ice sheet (Otto-Bliesner et al., 2006).

The LIGM warming was observed to be much more pronounced in Asia than global level. For example, pollen records obtained in northern Asia suggested that air temperatures were higher during the LIGM by more than 10 °C in winter and 4–8 °C in summer in northern Siberia and 2–6 °C in winter and 1–2 °C in summer in the Lake Baikal, and precipitation was about 100–150 mm above the modern values with a spread of Taiga (Grichuk, 1969; Rindzyunskaya and Pakhomov, 1977; Frenzel et al., 1992; Lozhkin and Anderson, 1995; Velichko et al., 1998; Tarasov et al., 2005). The warmer Asian climate during the LIGM is also supported by the enhanced Asian monsoon reconstructed by the analysis of stalagmites from Dongge Cave (Yuan et al., 2004) and increased precipitation in the lake Baikal (Granoszewski et al., 2005).

In order to investigate the causes of the climate change in the LIGM, several lines of numerical experiments were performed. Using CCM1 atmospheric general circulation model (AGCM) coupled with mixed layer ocean model, Harrison et al. (1995) obtained warming by more than 8 °C in northern Scandinavia and Beringia over the Arctic in northern winter during the last interglaciation associated with the

*Corresponding author: seongkim@kopri.re.kr

change in the extent and thickness of sea ice, but they obtained cooling in most regions of Siberia. In summer, however, they obtained the warming by more than 8 °C at latitudes around 60°N over Asia. Using ECHAM-1/LSG coupled atmosphere–ocean GCM, Kubatzki et al. (2000) and Montoya et al. (1998, 2000) obtained the surface warming by more than 4 °C in central Asia in northern summer, but they obtained the cooling by 2–3 °C in southern Asia in northern winter. More recently, using ECHAM4 coupled to HOPE-G model, Groll et al. (2005) obtained a slight warming over northern Asia and substantial warming by more than 2 °C in northern Europe in winter in the LIGM, which is in a better agreement with the observed proxy data. They and Kaspar et al. (2005) attributed the simulated warm European climate in winter to the increased westerlies and reduced sea ice extent.

These previous model studies have provided useful information on large-scale LIGM climate condition. During the LIGM summer, all model obtained the warming in the northern hemisphere including Asia and the summer warming is consistent with proxy estimates. However, in winter, simulated LIGM climate varies from model to model, especially over Asia/Arctic. For example, some models obtained a cooling over northern Asia in the LIGM simulations, other models obtained slight warming. The latter agrees better with proxy estimates, but the degree of surface warming is substantially underestimated. Moreover, the cause of anomalous winter warming over northern Asia remains uncertain and has not been analyzed. Because the anomalous response in northern Asia for the LIGM conditions could provide information that help understand the climate response under the future global warming, a proper understanding on how climate system responds to the different external forcing is important.

The purpose of this study is to investigate the climate response over Asia to the change in the LIGM orbital conditions and to examine how much the change in orbital parameters illustrate the total climate change obtained by proxy estimates. Because the seasonal climate response is quite distinct and strongest to the change in orbital parameters in the LIGM as illustrated later, we focus on the climate response to the change in orbital parameters.

2. MODEL DESCRIPTION AND EXPERIMENTS

We performed simulations with the NCAR CCM3.10.11 atmospheric general circulation model with 3.6.6 physics. This model is easily accessible and has been proved to be quite stable. The CCM3.6.6 includes a capability to calculate earth's orbital parameters, screen height temperature, the algorithm to calculate solar zenith angle. As a global spectral model, CCM3 includes 18 levels in a hybrid vertical coordinate that is terrain-following at the surface and reduces to a pressure coordinate in the upper atmosphere

with the model top at 2.9 hPa. The CCM3 atmospheric general circulation model used in this study has horizontal resolution at T42 truncation. The transform grid has 128×64 cells, with a typical grid size of about 2.8°. More detailed physical processes are represented as described in detail by Kiehl et al. (1998 a, b). The CCM3 includes a comprehensive model of land surface processes known as the NCAR Land Surface Model (LSM; Bonan, 1998).

Two experiments are performed. The first simulation, referred to as MOD, features the modern conditions, namely ocean is forced by prescribed, climatologically-averaged, monthly sea–surface temperatures (SSTs) and sea ice distributions provided by NCAR (<http://www.cgd.ucar.edu/>), atmosphere CO₂ concentration is 355 ppmv, and present land mask and topography are used. We specified the SST and sea ice boundary with observed climatological values.

In the second experiment, referred to as LIGM, we applied orbital parameters of the LIGM (Table 1). Earth's orbital parameters are composed of eccentricity, obliquity, and precession. The eccentricity is a measure of ellipticity of the orbit for the earth's revolution circle around the sun and has a period of 100,000 and 400,000 years. The obliquity (or axial tilt) is a measure of earth's tilt angle with respect to the plane of the earth's orbit and varies from 22.1° to 24.5° with a period of 41,000 years. The precession is a change in the orientation of the rotation axis of the earth and has 19,000 years and 23,000 years. As listed in Table 1, the eccentricity is almost the same and the obliquity is slightly larger in the LIGM. The longitude of perihelion (the time when the earthsun distance becomes shortest) is about 189 degree out of phase compare to that of present. This indicates that the earth was closest to the sun in northern hemisphere summer rather than in winter as today. The atmosphere CO₂ concentration was reduced by 10 ppmv from the present level because Petit et al. (1999) suggested the atmospheric CO₂ concentration of about 270 ppmv, which is 10 ppmv lower than the level of pre-industrial (280 ppmv). Because the atmospheric CO₂ concentration in the LIGM is almost the same as that of the pre-industrial, its effect on the climate change in the LIGM might be negligible. Because we are aiming at investigating the role of orbital parameters on the seasonal climate response over Asia for the LIGM, we keep the SST conditions same as present. Since we used the same SST and sea ice distribution for both periods, there would be an underestimation of surface temperature over the Arctic areas. Using the CCSM coupled AOGCM, Otto-Bliesner et al. (2006) obtained the

Table 1. Orbital conditions for the MOD and LIGM experiments

Parameter	Experiment	
	MOD	LIGM
Eccentricity	0.01670°	0.0397°
Obliquity	23.441°	23.922°
Lon of Perihelion	102.72°	292.03°

Arctic sea ice reduction by 50% in summer and the reduced sea ice led to simulated warming of the Arctic Ocean by about 2 °C.

3. RESULTS

The model was integrated for 15 years and the last 10 years were analyzed. Since we use the atmosphere only general circulation model with specified sea surface conditions, 15 years are enough for the atmosphere to adjust as shown in the time variation of annual mean surface air temperature (SAT) averaged globally and over Asia from 30° to 190°E and from 10°N to 80°N for the MOD and LIGM (Fig. 1). The SAT fluctuates interannually, but there is no climate drift with time for both MOD and LIGM experiments. We analyzed the January, July, annual mean quantities over the Asia continent because the observed proxy

data are available in those time periods only. Using the single month will slightly underestimate the amplitude of climate change in the LIGM due to calendar mismatch as shown in Figure 1 and also noted in a previous study (e.g., Joussaume and Bracconot, 1997) by the insolation forcing difference of the two periods, but its effect is relatively small.

3.1. Global and Asia Mean Response

With LIGM conditions, the SAT slightly increases in northern summer and slightly reduced in northern winter, indicating the larger seasonal contrast than today. This change is associated with the change in orbital parameters. The change in the timing of perihelion increased the seasonal insolation contrast in the northern hemisphere and this effect was amplified by the higher eccentricity. In addition, the increased axial tilt led to the increase in summer insolation at high northern latitudes and reduction in winter insolation at mid latitudes. The overall effect of orbital configurations at the LIGM was the increase in summer insolation in the northern hemisphere, especially in middle and high latitudes and the decrease in winter insolation, especially at low latitudes.

Table 2 summarizes the regional mean quantities averaged over the Asia land simulated in the MOD and LIGM experiments. In the LIGM, the area-mean surface temperature (SAT) at 2-m screen level increases in July by about 2.97 °C and decreases in January by 0.76 °C compared to the MOD experiment. The increase in SAT in July is largely offset by its reduction in January and other months and eventually the annual-mean surface temperature is slightly reduced in the LIGM by 0.46 °C over Asia land. The reduction in annual-mean surface temperature is also obtained by previous LIGM simulations. Using ECHAM/LSG and CLIMBER-2, Kubatzki et al. (2000) obtained the annual mean temperature reduction in the ECHAM/LSG and CLIMBER-2 by 0.3 °C and 0.7 °C, respectively, over the northern hemisphere land.

The surface temperature change in the LIGM compared to the MOD is predominantly due to the change in insolation. As listed in Table 1, the eccentricity of the earth's orbit and obliquity were slightly greater in the LIGM, and the perihelion occurred in July in contrast to the present when the perihelion occurred in January. This means that at 126 kBP the earth received more energy in northern summer and less in northern winter. This feature is well reflected in the change in incoming solar radiation (insolation) (Table 2). In July, the insolation increases by $\sim 47 \text{ Wm}^{-2}$, which is about 10% of present value. In January, on the other hand, insolation decreases by $\sim 14 \text{ Wm}^{-2}$ (about 9%).

In order to find out the role of orbital parameters on the surface temperature change, we investigate the change in energy budget at the surface. Following Peixoto and Oort

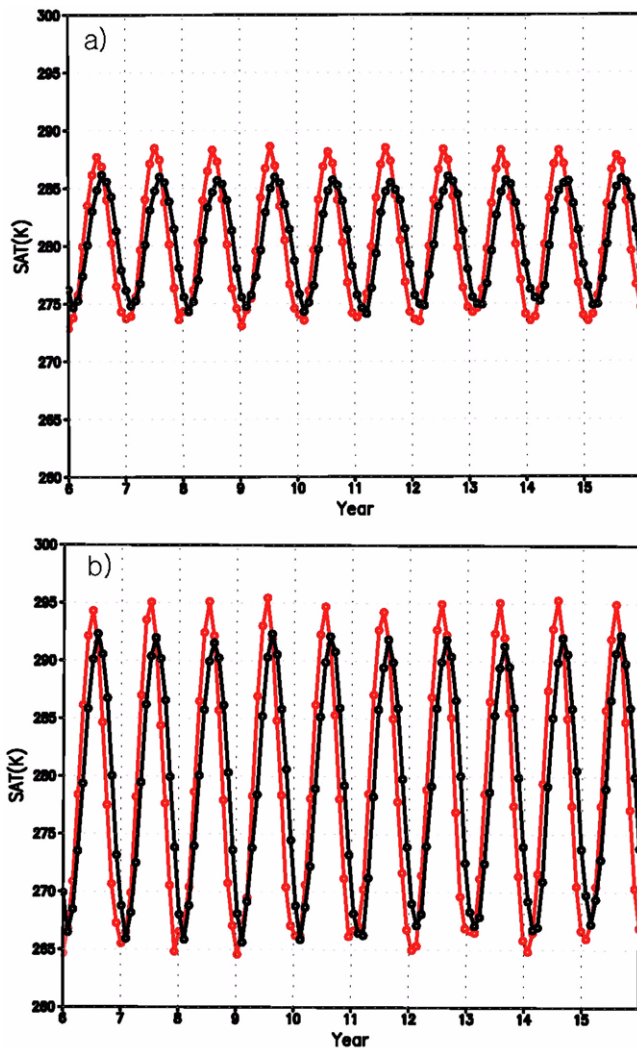


Fig. 1. Time variation of the annual mean surface air temperature (SAT) averaged over a) global and b) Asia domain (10°N to 90°N; 30° to 190°E) for the MOD (black) and LIGM (red) simulations.

Table 2. January, July, and annual mean quantities from MOD and LIGM simulations averaged over Asia land (30°–190°E; 10°–80°N). Radiative heat fluxes in parentheses are the values in the case of clear sky. The bold face indicates values statistically significant at 95% confidence level. For the underlined values, statistical significance is not estimated because there is no interannual variation

	MOD	LIGM	LIGM-MOD
Surface Temperature (K)			
Ann	279.40	278.94	–0.46
Jan	266.43	265.67	–0.76
Jul	291.94	294.91	2.97
Insolation (Wm ^{–2})			
Ann	312.34	312.65	<u>0.31</u>
Jan	162.90	149.16	<u>–13.74</u>
Jul	460.90	507.52	<u>46.62</u>
Short-wave (Wm ^{–2})			
Ann	136.18(181.85)	138.42(180.86)	–3.76(–0.99)
Jan	68.66(85.51)	61.26(77.09)	–7.40(–8.42)
Jul	201.41(284.67)	209.51(310.42)	8.10(25.75)
Long-wave (Wm ^{–2})			
Ann	–67.27(–100.71)	–63.58(–97.85)	3.69(2.86)
Jan	–57.69(–97.94)	–56.08(–97.62)	1.61(0.32)
Jul	–69.44(–97.00)	–62.12(–88.70)	7.32(8.30)
Latent (Wm ^{–2})			
Ann	–40.66	–43.34	–2.67
Jan	–12.34	–11.13	1.21
Jul	–76.24	–90.66	–14.42
Sensible (Wm ^{–2})			
Ann	–26.22	–23.58	2.64
Jan	–6.83	–1.71	5.12
Jul	–44.93	–44.21	0.72
Cloud Fraction(5)			
Ann	53.50	55.46	1.96
Jan	55.23	56.01	0.78
Jul	55.95	61.67	5.72
Precipitation (mm/day)			
Ann	2.04	2.22	0.18
Jan	0.93	0.92	0.01
Jul	3.52	4.47	0.95

(1992) and Boer (1993), the energy budget at the surface layer of land is written as

$$C_* \frac{\partial T}{\partial t} = S + F + LE + H,$$

where C_* is the heat capacity of a layer, T the temperature, S the net short-wave ($S = (1 - \alpha)S^\downarrow$, where S^\downarrow the incoming solar radiation and α the surface albedo), F the net long-wave radiative heat fluxes ($F = F^\downarrow - \sigma T^4$, where F^\downarrow is the incident and $-\sigma T^4$ the emitted long wave radiation at the surface, where σ is StefanBoltzmann constant ($5.67 \times 10^8 \text{ W m}^{-2} \text{ K}^{-4}$)), and LE the latent heat fluxes (L is latent heat of evaporation), and H is the sensible heat fluxes at the land

surface. Note that the ground heat flux term involved in melting snow and ice or freezing water is not included in the equation because the term is negligible over a long-term period. In equilibration, the rate of change term is small and the difference in heat budget terms between LIGM equilibrium and MOD climates is $\delta S + \delta F + L\delta E + \delta H = 0$. Sign convention is that all fluxes are positive if they act to warm and negative if they act to cool the land surface.

With LIGM conditions, the net short-wave radiative heat flux increases by 8.1 Wm^{-2} (about 4%) in July and acts to warm the surface. In January, on the other hand, the short-wave heat flux is reduced by 7.4 Wm^{-2} (about 11%) and acts to cool the surface. This result is not consistent with the change in the insolation because its increase in July is much larger than the amount of its decrease in January by more than three times. The difference between the insolation change and short-wave heat flux at the surface is due to the absorption in the atmosphere. In January, the net short-wave radiative heat flux is reduced by about 20% through atmosphere in both the MOD and LIGM, while in July it decreases by about 30% in the MOD and by 33% in the LIGM. The larger reduction in the short-wave heat flux in July than in January is mainly associated with the increase in cloud amount. Overall, the annual mean short-wave heat flux decreases slightly by about 4 Wm^{-2} (~3%) and is such as to cool the surface in the LIGM over Asia.

The change in surface temperature in response to the change in the net short-wave radiative heat flux consequently modifies the long wave radiative and turbulent heat fluxes and reaches the new energy balance. In the LIGM, there is a slight increase in the area-averaged net long wave radiative heat flux in January associated with the reduction in SAT. However, in July the area-averaged long wave heat flux increases substantially regardless of the increase in the area-mean SAT shown above and acts to warm the surface. The increase in July long wave heat flux is mainly due to the reduction of surface temperature over the southern part of Asia as shown later.

The reduced surface temperature in January leads to a reduction in evaporation and thus the latent heat flux, that is such as to warm the surface slightly. In July, on the other hand, latent heat flux increases substantially by about 14 Wm^{-2} (~18%) due to the surface warming, acting to cool the surface. The annual mean latent heat flux decreases slightly, acting to cool the surface. The sensible heat flux term is generally a loss term in heat budget. In January, the surface cooling leads to the reduction in sensible heat loss, but in July there is almost no change in the sensible heat flux. Overall, the change in sensible heat flux acts to warm the surface.

The change in surface temperature in the LIGM is reflected in the change in the total cloud amount and precipitation. The vertically integrated total cloud appears to increase in all season in the LIGM, especially in July. Precipitation changes very little in January and its change is statistically

the same as that of present, whereas it increases substantially in July by about 27% in the LIGM associated with the increase in SAT and cloud. The increase in summer precipitation over Asia land implies a stronger Asian summer monsoon.

3.2. Zonal-mean Monthly Response

Figure 2 displays the change in the zonally averaged monthly insolation and short-wave radiative heat flux at surface averaged from 30° to 190°E over land. As would be expected from the changes in orbital parameters, the insolation decreases substantially from September to November by more than 40 W m^{-2} in the north of 40°N and in December to January the maximum reduction occurs at low latitudes. From April the insolation begins to increase and the maximum insolation by more than 55 W m^{-2} occurs in the north of 35°N in June. The increase in the solar insolation

by more than 40 W m^{-2} is maintained until August from low to high latitudes.

The short-wave radiation is substantially reduced to about 50% of the insolation while reaching the surface through the atmosphere (Fig. 2b). While the largest change in the insolation occurs in high latitudes, the largest change in the short-wave radiative heat flux is found in low to mid latitudes. In October, the large reduction in the short-wave heat flux by more than 25 W m^{-2} is found in mid latitudes and in low latitudes in November. The substantial reduction of short-wave heat flux is even found in July at 20°–30°N that is due to the increase in cloud amount by more than 15% (not shown). The short-wave heat flux gradually increases from April and the maximum increase by more than 30 W m^{-2} is found from June to August from low to high latitudes.

The change in the short-wave heat flux at surface is broadly similar to that of surface temperature (Fig. 3a). From April

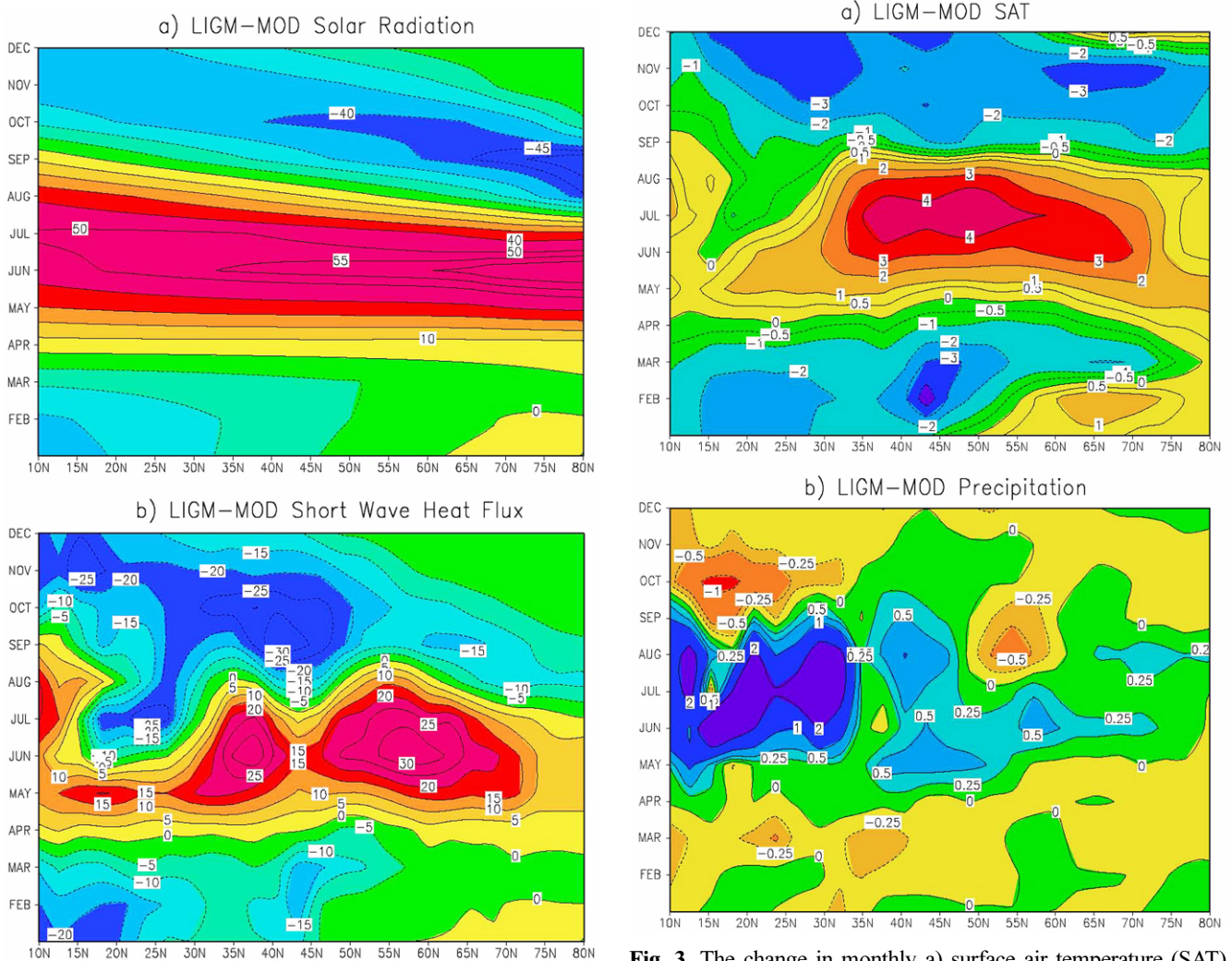


Fig. 2. The change in monthly a) insolation and b) the short-wave radiative heat flux between the MOD and LIGM averaged over Asia (30° to 190°E). Units are in W m^{-2} .

Fig. 3. The change in monthly a) surface air temperature (SAT) and b) precipitation between the MOD and LIGM averaged over Asia (30° to 190°E). Units are in C for SAT and mm day^{-1} for precipitation.

to September, the surface is warmer in the LIGM than present. The warming is especially large in mid latitudes where the surface temperature increases by more than 4 °C. In low latitudes, the warming is relatively small and even a slight cooling is found at 20°N due to the increase in cloud amount in the LIGM as shown later. From October to December and March, surface is colder than present from low to high latitudes in consistent with the reduction in short-wave heat flux. In January and February, surface cooling is found from low to mid latitudes, but surface warming by more

than 1 °C is obtained in high latitudes. This anomalous winter warming in high northern latitudes of Asia is in part illustrated by the change in the insolation and short-wave heat flux. However, the increase in insolation is less than 1 Wm⁻² and short-wave heat flux at surface is less than 0.5 Wm⁻², which is obviously not sufficient to illustrate such a relatively big surface warming completely. A relatively big change in incoming long wave heat flux and some circulation change around the Arctic in part are responsible for the winter surface warming as shown later.

Table 3. January, July, and annual-mean surface temperature and annual precipitation change between the LIGM and MOD derived from proxy records

No.	Location	ΔTemp Jan (°C)	ΔTemp Jul (°C)	ΔTemp Ann (°C)	ΔPCP ann (mm)	References
1	European Russia	4				Devyatova (1982); Grichuk (1984)
2	Boyarschina	6	1	4	0	Grichuk (1984)
3	Petrozavodsk	7	1	5	120	Devyatova and Starova (1970)
4	Il'inskoye	8	0	4	30	Grichuk et al. (1983)
5	Mironovka	1	-2	-1	300	Artyushenko (1970)
6	Levina Gora	10	0	5	0	Gorlova (1967)
7	Yakimanka	11	0	6	0	Metel'tseva and Sukachev (1961)
8	Mys Krotkova	2	-1	1	600	Arslanov et al. (1983)
9	Lia	0	0	0	0	Mamatsashvili (1975)
10	Posudichi	5	0	3	50	Gurtovaya and Faustova (1977)
11	Suvod'	11	1	5	50	Ivanova (1973)
12	Arkhangelsk	3	1	3	100	Pleshivtseva (1972)
13	Svyatoi Nos	2	1	1	100	Nikonov and Vostrukhina (1964)
14	Novaya Zemlya	5	7	6	50	Malyasova (1989)
15	Nadota	3	4	4	50	Rindzyunskaya et al. (1987)
16	Marre-Sale	3	8	5	200	Gurtovaya and Troitskiy (1968)
17	Lukovaya Protoka	7	2	5	260	Volkova et al. (1988)
18	Yeloguy	8	1	4	0	Gurtovaya (1987)
19	Bolshaya Rassokha	13	8	10	200	Nikol'skaya (1980)
20	NE Siberia	4	4~8		Wetter	Lozhkin and Anderson (1995)
21	West central Siberia	5~7	6~8		Wetter	Gudina et al. (1983); Grichuk (1984)
22	Lake Baikal	2~6	1~2		100	Tarasov et al. (2005)
23	Lower Yana-Kolyma	-12	4~8		wetter	Lozhkin and Anderson (1995)
24	Upper Kolyma / Indigirka	0~4	4		wetter	Lozhkin and Anderson (1995)
25	Yelon'	12	5	5	40	Giterman (1963)
26	Okhotsk Sea Coast	4	4		Wetter	Lozhkin and Anderson (1995)
27	Nikolai Gulf	4	3	1	200	Boyarskaya et al. (1978)
28	Vostok Gulf	0	0	0	0	Korotkiy et al. (1980)
29	Tumangan	0	0	0	0	Alekseev and Golubeva (1980)
30	Kamchatka	4	0	1	0	Skiba (1975)
31	NE Siberia, Lake Elgygytgyn	4	3		Wetter	Lozhkin et al. (2007)
32	Anadyr' Liman	-1	4	1	0	Muratova (1973)
33	Chukotka	-12	4~8		wetter	Lozhkin and Anderson (1995)
34	Kaktas	1	-3	-2	100	Chupina (1978)
35	Siberia		4~5		Wetter	Andreev et al. (2004)
36	Gornaya Subbota	5	0	3	100	Gurtovaya and Krivonogov (1988)
37	Kozyulino	7	0	4	150	Arkhipov et al. (1973)
38	Lake Baikal North	5	4	6	50	Rindzyunskaya and Pakhomov (1977)

With LIGM conditions, precipitation overall increases over Asia (Fig. 3b). The largest increase in precipitation is found from May to September south of 30°N. This implies that the Asian summer monsoon was enhanced in the LIGM as also obtained by previous model studies (e.g., Prell and Kutzbach, 1987; de Noblet et al., 1996). A substantial reduction in precipitation is found in tropics in northern winter, but there is little change in mid to high latitudes due to the lack of moisture source.

3.3. Geographic Response over Asia Continent

3.3.1. Surface temperature

We first examine how much the surface temperature was altered in the LIGM based on paleoclimate reconstruction. Table 3 lists January, July, and annual-mean surface temperature change and annual-mean precipitation change derived mainly from pollen and macrofossil records. The temperature change listed in Table 3 is displayed in Figure 4. The reconstructed proxy data show that in January the surface temperature increased substantially in most part of northern Asia north of 45°N. The temperature increase is especially large in the east Siberian Arctic coast such as the Taimyr coast, where the January temperature exceeds the present-day temperature by 13 °C. In western Siberian Arctic and northern Eurasia, a more uniform warming by 4–6 °C is recorded. In central part of West Siberia and south of middle Siberia the warming ranges from 6 to 8 °C. A warming by 4 °C was reconstructed along the coast of the Sea of Okhotsk, but a substantial cooling by 12 °C was obtained in the eastern Siberia. Towards south, the January warming diminishes and a small cooling was obtained in the middle latitudes.

In July, the degree of the reconstructed surface warming is overall smaller than that in January (Fig. 4b). The largest warming was again obtained in the Arctic regions such as the Taimyr and Yamal peninsulas where the warming was greater than 8 °C. The degree of warming is smaller in the eastern Siberia by 4–5 °C and by 1–4 °C in western Siberia. In the sub-Baikal region and along the coast of the Sea of Okhotsk, the temperatures were 3–4 °C higher than present. In western Asia between 50°–60°N, the July temperatures were close to the present day and south of 50°N, near the Black Sea and the south-eastern Kazakhstan, small cooling was recorded.

Overall, the mean annual temperatures in the LIGM exceeded those of the present day in the northern Asia/Arctic north of 50°N (Fig. 4c). The surface warming increases towards the north and reaches 10 °C in the coastal region of Taimyr, which is about halfway between January and July. In Eurasia and northern Asia, the annual mean surface warming ranges 3–6 °C, but along the coast of eastern Siberia including the Amur river, Sakhalin island, the annual-mean temperature increase is small by about 1 °C. In north-

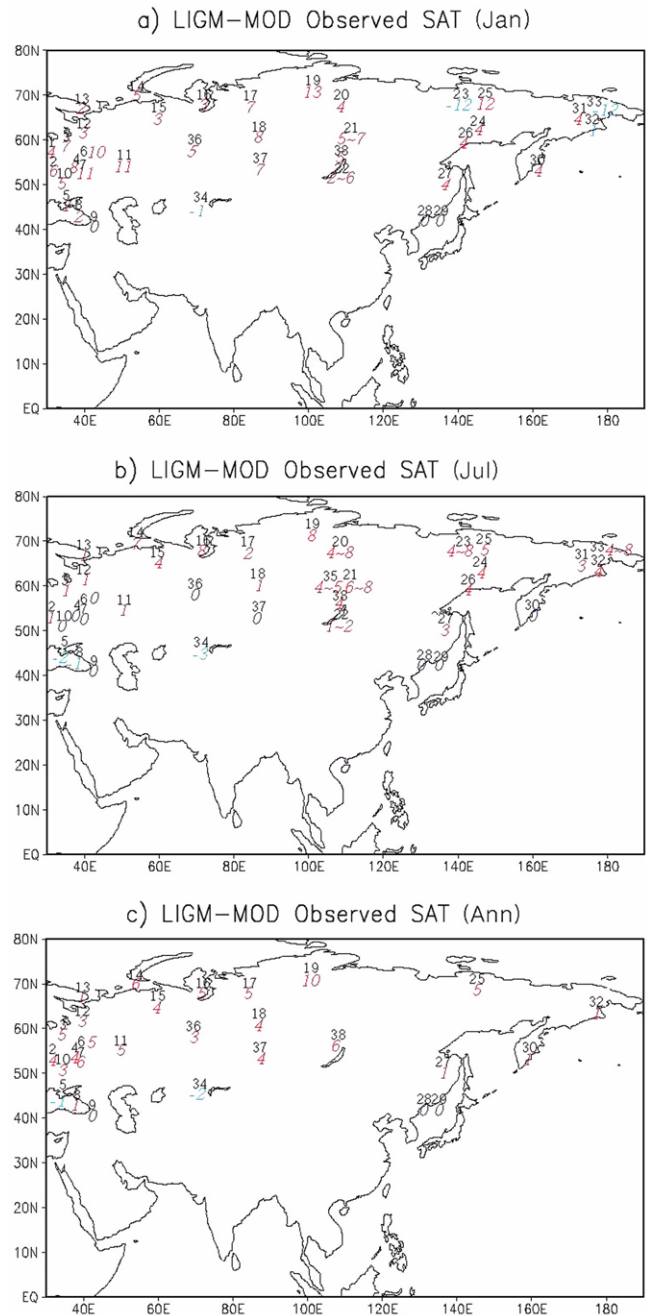


Fig. 4. Geographic distribution of the change in observed surface air temperature (SAT) between the LIGM and modern conditions derived from proxy records for a) January, b) July, and c) annual-mean. Units are in °C.

ern Kazakhstan, the small cooling is obtained.

Figure 5 displays the geographic distribution of the change in the simulated SAT between the LIGM and MOD in January, July, and annual mean. In January, the marked warming is simulated over northern Asia, eastern Eurasia, and the Arctic. The largest warming is found over the Barents Sea by more than 3 °C, which is about 2 °C lower than proxy estimates. In the Taimyr and Yamal peninsulas, the simu-

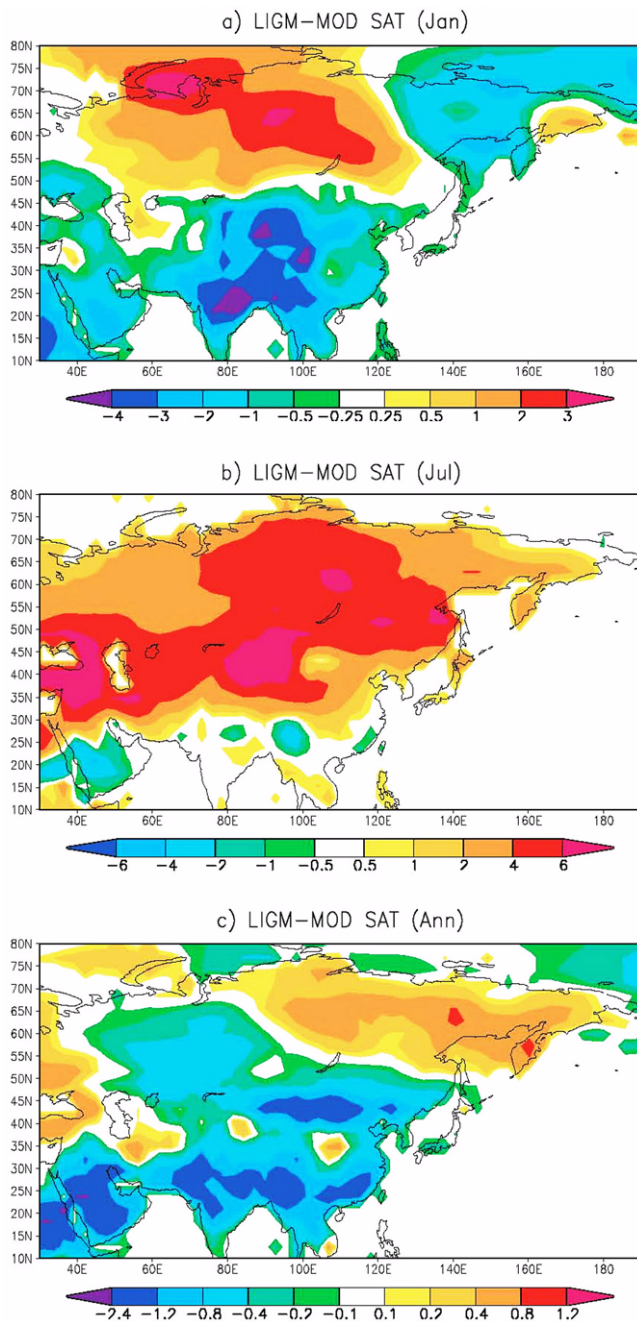


Fig. 5. Geographic distribution of the change in simulated surface air temperature (SAT) between the LIGM and MOD for a) January, b) July, and c) annul-mean. Units are in $^{\circ}\text{C}$.

lated surface warming is less than 2°C , which is substantially lower than the proxy estimates (13°C). As mentioned in the introduction, Harrison et al. (1995) obtained the surface warming by more than 8°C in the Arctic including the Barents Sea, which is close to the degree of warming suggested by proxy estimates. This indicates the critical role of the sea ice albedo feedback in reproducing the substantial warming over northern Siberia and Arctic. In eastern Siberia and low to mid latitudes south of 50°N , the surface cool-

ing is obtained. The surface cooling is especially large over the Tibetan Plateau by more than 4°C . Even though the signal is mixed, the surface cooling signature in eastern Siberia and in mid latitudes is also found in the proxy estimates (Fig. 4a).

The simulated surface temperature change pattern in January is broadly consistent with the proxy reconstruction such as the warming in northern Asia and cooling in eastern Siberia and low latitudes, but the degree of surface warming in the simulation is substantially lower than those of the reconstructions. Some previous LIGM simulations also obtained the surface warming in winter over northern Asia, but the degree of surface warming is substantially less than proxy estimates even using coupled AOGCMs. For example, Harrison et al. (1995) obtained the surface warming by about 2°C using CCM1 with mixed layer ocean, Montoya et al. (2000) and Groll et al. (2005) by less than 1°C using AOGCM. Note, however, that a direct comparison between the proxy estimates and simulated results is difficult because the model results represent a broadly averaged quantity, while the proxy records often represents a relatively small area and may be related to a regional phenomena. Overall, using CCM3 AGCM the change in orbital parameters for the LIGM illustrates less than 50% of the total surface temperature change in January in northern Asia.

In July, the surface warming is obtained in most parts of Asia except over low latitudes where a slight cooling is simulated. The surface warming is especially large in the north of the Tibetan Plateau and Middle East Asia where surface temperature increases by more than 6°C . In low latitudes south of 30°N , on the other hand, surface temperature decreases slightly. The simulated warming in July is broadly consistent with the proxy reconstruction, even though detailed features are different. First, largest warming was obtained in the northern high latitudes in the proxy reconstruction, but in the simulation the greatest temperature increase is found over middle latitudes between 40° – 50°N . Using the CCSM coupled AOGCM, Otto-Bliesner et al. (2006) obtained the maximum warming at about 40°N by more than 6°C as in this study, while they obtained more realistic surface temperature change over the Arctic Ocean by including ocean dynamics and sea ice. Second, in the simulation the surface cooling is obtained in low latitudes south of about 30°N , but in the proxy records the cooling begins from about 50°N . Using ECHAM-1/LSG and ECHO-G coupled AOGCM, Montoya et al. (2000) and Groll et al. (2005) obtained slight surface cooling over India and southern Saudi Arabia as in this study. This indicates that the mismatch in the location of the surface cooling is not due to the representation of ocean circulation and sea ice feedback. Third, the degree of simulated surface warming is slightly lower than those of reconstructions. Overall, the change in orbital parameters largely illustrates the degree of surface warming in northern Asia in July, although there is

a mismatch in the location of maximum warming between the simulation and proxy estimates.

The seasonal contrast becomes larger in low and mid latitudes of Asia in the LIGM. The larger seasonality over Asia during the last interglacial period was also obtained by proxy coral records in Ryukyu Islands of the northwest Pacific (Suzuki et al., 2001) and in the northern Red Sea of Middle East Asia (Felis et al., 2004) and previous model studies (Kubatzki et al., 2000; Montoya et al., 2000). Overall, the change in orbital parameters largely illustrates the degree of surface warming in northern Asia in July.

The annual-mean surface temperature slightly decreases in low to mid latitudes and slightly increases in north-eastern Asia and Eurasia. The surface warming in northern and north-eastern Asia and part of Eurasia is consistent with the proxy reconstructions. However, the degree of the annual-mean temperature change in the simulation is much lower than those of proxy reconstructions as in the case of January and July because in the simulation the surface warming in July is largely offset by the surface cooling in January, especially in mid latitudes. This indicates that the change in orbital parameters is not sufficient to account for the change in LIGM surface temperature and other conditions such as ocean circulation and sea ice must be included.

3.3.2. Surface energy budget

In order to find out the causes of the surface temperature response, we examine the change in surface energy budget. Figures 6a and b display the geographic distribution of the difference in the net short-wave radiative heat flux (δS) in January and July. In January, the short-wave radiative flux change acts to cool the surface due to the decreased insolation over most Asia except for south-eastern China, where the short-wave radiation acts to warm the surface. There is comparatively little change in short-wave heat flux over northern high latitudes of Asia and the Arctic. The overall reduction in short-wave radiation in low to mid latitudes is consistent with the surface cooling in those regions of Asia shown in Figure 5a. However, a substantial surface warming was obtained, even though there is little change in the shortwave radiative heat fluxes in high latitudes.

In July, the short-wave radiative heat flux is such as to warm the surface, except in south Asia, north-eastern China, and part of Saudi Arabia, where the short-wave heat flux is reduced and acts to cool the surface. The reduction of the short-wave radiative heat flux in low latitudes in spite of the increase in insolation is partially due to the increase in cloud amount as shown later. The surface temperature change in July is overall consistent with the change in the short-wave heat fluxes, except over the Northeast Asia where a reduction in the short-wave radiative heat flux is obtained, while a substantial warming is obtained (Fig. 5b).

These results indicate that the change in the short-wave heat fluxes is not enough to illustrate the change in the sur-

face temperature. In addition to the change in the net short-wave heat fluxes, the change in the incident long wave heat fluxes modifies the surface temperature. Figures 6c and d show the change in the downward long wave heat flux (δF^{\downarrow}). In January, the downward long wave heat flux increases in northern Asia, whereas it decreases over southern Asia and eastern Siberia. The change in the downward long wave heat flux is overall consistent with that of the surface temperature, indicating its important role in illustrating the January surface temperature change. In July, the downward long wave heat flux overall increases and acts to warm the surface, especially middle east to northeast Asia.

The change in surface temperature subsequently modifies the turbulent (latent and sensible) heat fluxes. Figures 6e and f show the geographic distribution of the change in the turbulent heat fluxes between the two periods. In January, the change in latent heating is such as to warm the surface over most areas, reflecting a reduction in evaporation associated with the surface cooling mainly at low latitudes. In July, the change in the turbulent heat fluxes largely decreases in most of Asia and acts to cool the surface, except over India and North-eastern China. The reduction in the turbulent heat fluxes is mainly due to the increase in evaporation in the LIGM (not shown), associated with the surface warming.

3.3.3. Cloud

The change in the net short-wave radiation and incident long wave radiation modifies the surface temperature. These radiative heat fluxes can be modified through an absorption or scattering by impurities in the atmosphere. One of the most important factors in determining the amount of incident short-wave and long wave radiation is the cloud, which plays a very important role in the radiation balance and thus in climate. The cloud affects albedo, absorptivity, and transmissivity of the incident radiation.

Figure 7 shows the change in high, mid, and low cloud in percent between the two experiments. The high, mid, and low clouds are averaged above 200 hPa level, between 200 hPa and 500 hPa, and below 500 hPa level. In January, The high cloud increases in the northern Siberia and Arctic Ocean and low latitudes including Saudi Arabia, India, and south Asia, but changes very little in mid latitudes. The mid and low clouds increase largely over northern Asia/Arctic including the Kara Sea and over middle east Asia, but they substantially decrease in eastern Siberia and over India. The change in the high cloud in the Arctic and the mid and low cloud amount is broadly consistent with the change in the downward long wave heat fluxes (Fig. 6c), indicating the important role of the cloud in surface temperature change in January.

In July, the cloud amount overall increases in low latitudes in all levels (Fig. 7). The overall increase in clouds in low latitudes are consistent with the reduction in the short-wave heat flux (Fig. 6b) and surface cooling (Fig. 5b). The

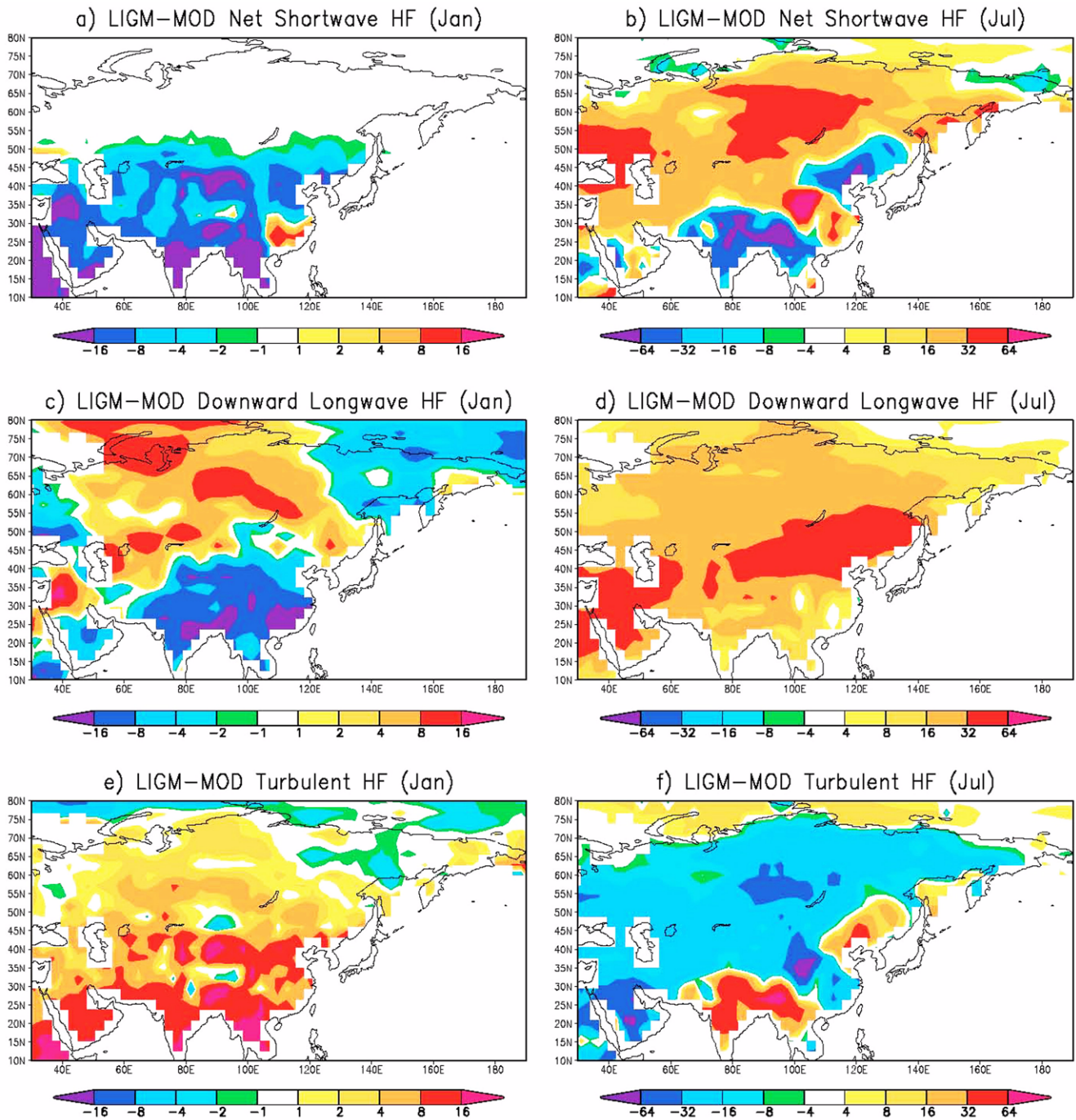


Fig. 6. Geographic distribution of the change in net short-wave radiative heat fluxes for a) January, b) July, downward long wave radiative heat fluxes for c) January, d) July, turbulent heat fluxes for e) January, f) July. Units are in W m^{-2} .

cloud amount increases in mid latitudes of east Asia at all levels. This helps block the shortwave radiative heat fluxes, but increases the long wave heat fluxes. Eventually, they offset each other and surface temperature change is relatively small. In middle latitudes, the increase in the mid and low level clouds is consistent with the marked increase in long wave heat fluxes and surface warming, while in high latitudes the reduction of low level clouds are consistent with

the marked increase the shortwave radiative heat fluxes and surface warming.

3.3.4. Arctic oscillation

The Asian climate over mid to high latitudes is governed by the Arctic Oscillation (AO), especially in winter. The AO is the leading mode of northern hemisphere atmospheric variability from troposphere to lower stratosphere

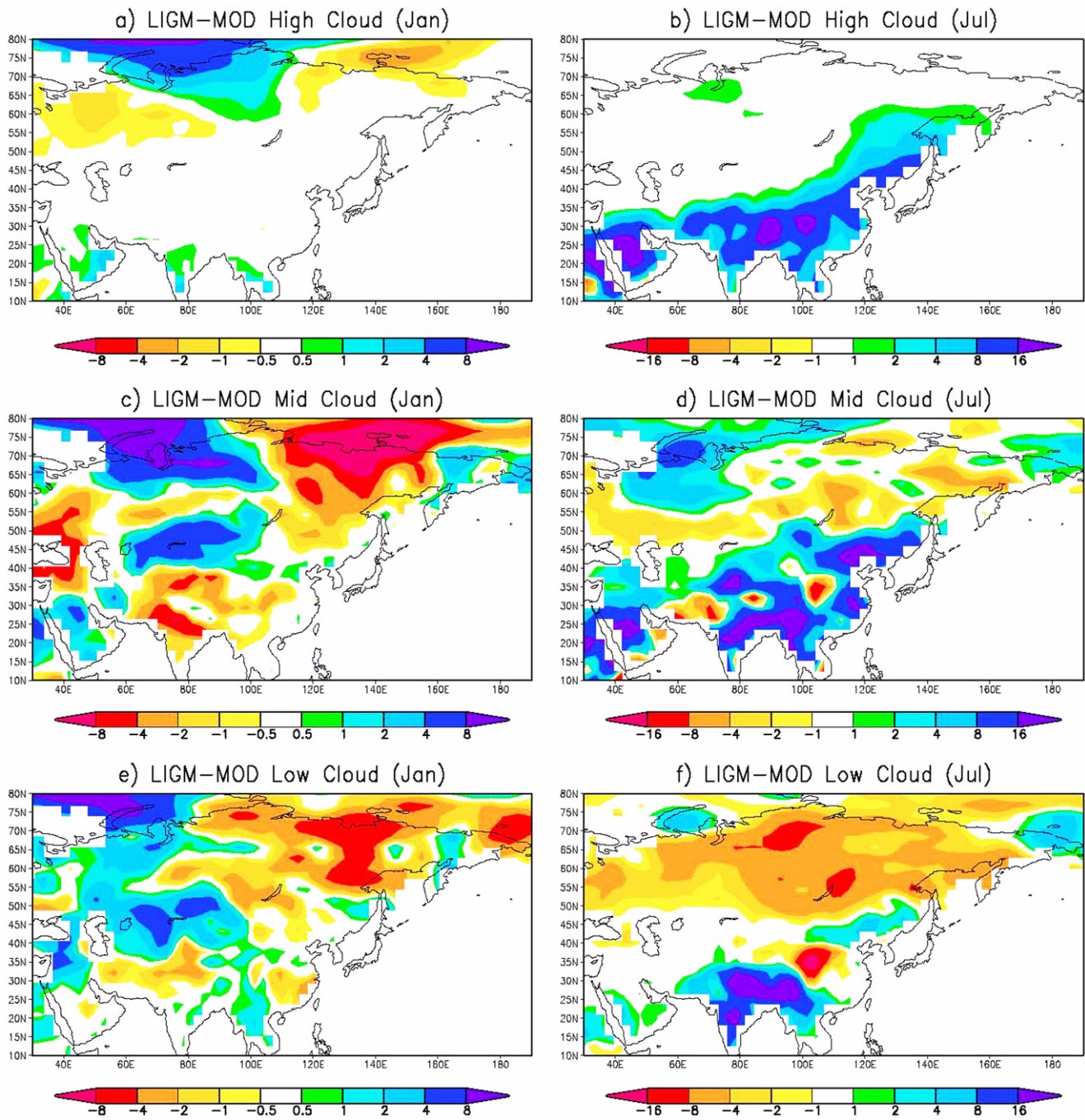


Fig. 7. Geographic distribution of the change in high level (above 200 hPa) cloud for a) January, b) July, mid level (200–500 hPa) for c) January, d) July, and low level (below 500 hPa) cloud for e) January and f) July. Unit is in %.

(Thompson and Wallace, 1998, 2000). For example, in high AO index years a warmer climate, smaller weather variance, less frequent cold surges, and lighter sea ice conditions over Asia are observed during winter and spring (Gong et al., 2001, 2007; Wu and Wang, 2002; Gong and Ho, 2004; Jeong and Ho, 2005). The AO can be modulated by the presence of snow over the Tibetan Plateau (Lu et al., 2008) and its intensity appears to be weaker during the Last Glacial Maximum (Lu et al., 2010). Here we investigate the change in

the AO in the LIGM and its influence on the surface temperature change over Asia/Arctic. The AO analysis includes only January because the AO is most active during northern winter.

In describing the patterns of atmospheric variability, the empirical orthogonal function (EOF) is commonly used. Figure 8 shows the leading EOF of January sea level pressure (SLP) simulated in the MOD and LIGM with the observed for 1980–2000 period. The AO pattern simulated

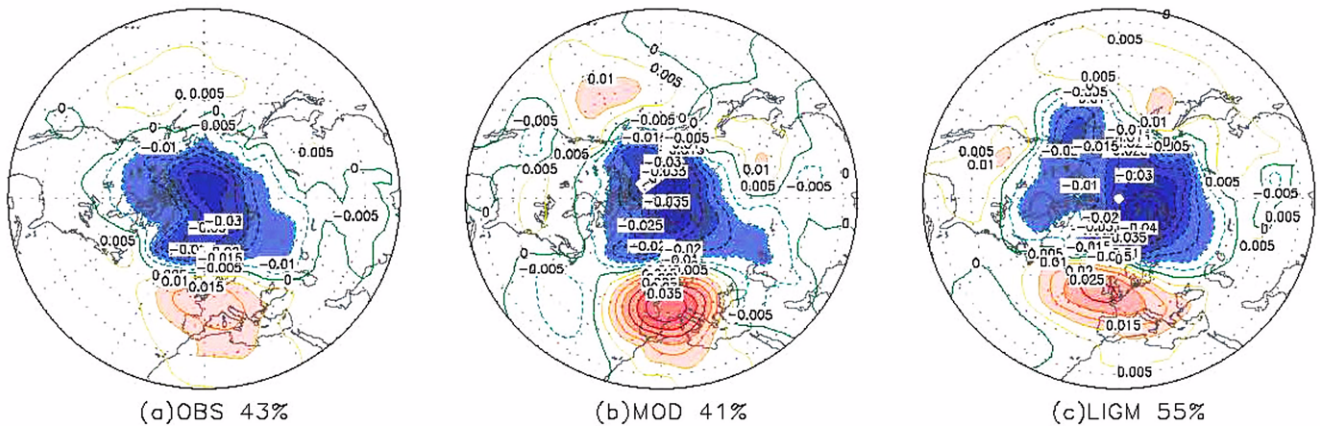


Fig. 8. Geographic distribution of the leading EOF for January SLP in a) observed (OBS) for 1980–2000 period, simulated in the b) MOD, and c) LIGM. Percentages of explained variance are shown at the top of each panel. The absolute values greater than 0.01 are shaded.

in the MOD is similar to that of the observed with a stronger dipole over the North Atlantic corresponding to the North Atlantic Oscillation (NAO) and a weaker dipole over the North Pacific. The leading EOF mode illustrates 41% of total variance in the MOD, which is similar to the observed (43%). In the LIGM, the leading EOF illustrates the total variance larger (55%) than that in the MOD. The positive loading in the North Atlantic and North Pacific becomes weaker, but the negative loading over the Arctic appears to be reduced. The weakening of the positive loading over the North Pacific in winter of the LIGM is also obtained by Groll et al. (2005) using ECHOG OAGCM. Analysis indicates that the amplitude of the AO becomes stronger in the LIGM than in the MOD, implying that intensity of the AO increased in the LIGM. The stronger AO intensity in the LIGM simulated in this study is consistent with previous model results (Groll et al., 2005; Hall et al., 2005).

In order to investigate the impact of the AO on surface temperature, we regressed the SAT on the standardized AO index (Fig. 9). In the MOD, the positive AO is associated with the surface warming over high latitudes of Asia and Eurasia including the Arctic, whereas in eastern Siberia and mid latitudes the positive AO is associated with the slight cooling. This pattern is due to the warm air advection associated with stronger westerlies as shown by Thompson and Wallace (2000). In the LIGM, the larger warming over northern Asia/Arctic and a larger cooling in eastern Siberia are obtained. This is consistent with the strengthened AO polarity in the LIGM. This result indicates that the change in AO and associated heat advectons plays a partial role in illustrating the surface warming in northern Asia/Arctic in January in the LIGM.

3.3.5. Precipitation

The change in cloud amount is associated with the change in precipitation. Figure 10 compares the annual precipitation reconstructed from pollen records with the simulation.

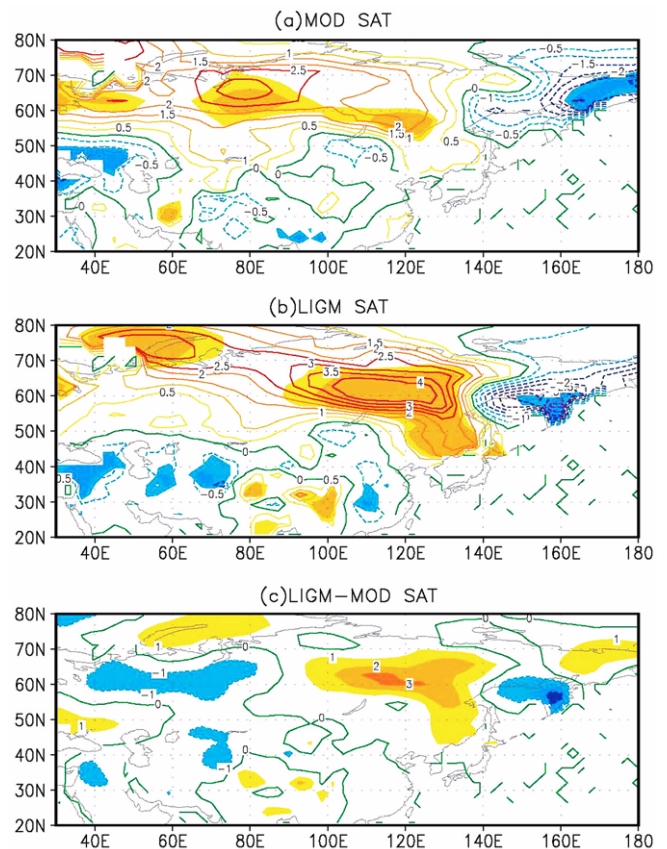


Fig. 9. Geographic distribution of the surface air temperature (SAT) regressed on the standardized AO index in the a) MOD and b) LIGM, c) the difference between the LIGM and MOD. Unit is K per standard deviation of the respective index time series. Regression coefficients are shown as contours. Correlation coefficients at 90% and 95% confidence level are shaded in A) and B). Differences greater than 1 K are shaded in c).

The proxy estimation shows that in the LIGM precipitation substantially increased by 50 to 200 mm in middle and northern Asia and its distribution was more uniform than

present. Within the mid latitude belt of the East European plain, annual precipitation changed relatively little from the present-day by about 7–8% (50 mm). In some areas such as in north-western Asia, almost no change in precipitation was obtained, whereas in the Karelia (120 mm) and the Kola Peninsula (100 mm) near the Barents Sea a greater increase in precipitation was reconstructed. The substantial increase in precipitation is found over western Siberia/Arctic by more than 200 mm.

An increase in precipitation in the arid regions at present is of special interest. For example, in northern Kazakhstan and Middle East Asia the annual precipitation in the LIGM exceeds modern values by 100 mm. On the whole, in the latitudinal belt south of 55°N where precipitation is insufficient at present, a considerable increase in precipitation occurred during the LIGM, in particular to the west of this belt. In the northern Black Sea coastal region, the precipitation increased by 600 mm.

In the simulation, the annual precipitation appears to increase in northern Asia/Arctic, especially western Siberia, the Kara Sea, and far eastern Siberia where precipitation increases by more than 40 mm (Fig. 10b). This feature is consistent with the proxy reconstructions, even though the degree of the simulated precipitation change is much smaller than that in the proxy records, especially in the central Siberia including the coastal region of Taimyr. Towards south in the latitude belt around 55°N precipitation tends to decrease, especially in western Asia.

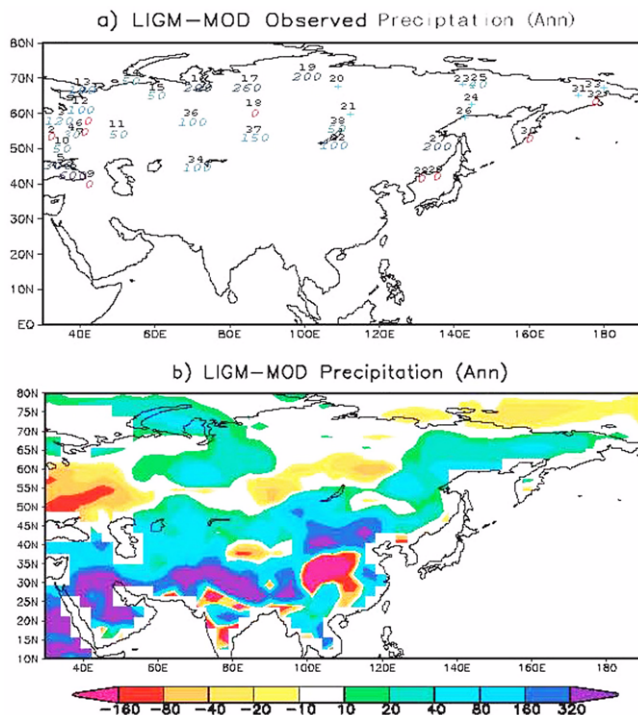


Fig. 10. Geographic distribution of the change in annual a) reconstructed from proxy records and b) simulated precipitation. Units are in mm.

low latitudes precipitation substantially increases, especially over now arid region of Saudi Arabia and north of India where precipitation exceeds more than 300 mm. The increase in precipitation over now arid regions such as Saudi Arabia and Middle East Asia is associated with the increase in moisture transport by the stronger southwest winds in July and southerly winds in January as illustrated later. The increase in precipitation in latitudes between 40°–50°N including the Lake Baikal is consistent with the proxy records. South of this latitude belt it is hard to determine whether the simulated increase in annual precipitation is realistic due to the lack of quantitative reconstruction of proxy data. The change in oxygen isotope ratios of stalagmites retrieved from the Dongge cave in south China indicates an increase in precipitation during the LIGM, especially in summer (Yuan et al., 2004). Overall, both proxy records and simulation show the increase in annual precipitation over Asia in the LIGM.

Figure 11 displays the change in precipitation in January and July. In January, a slight increase is simulated over northern part of Middle East Asia such as Kazakhstan, the Kara Sea, and Far Eastern Siberia. The increase in precipitation in these regions is consistent with the proxy reconstructions (e.g., Velichko et al., 2007). Proxy records also

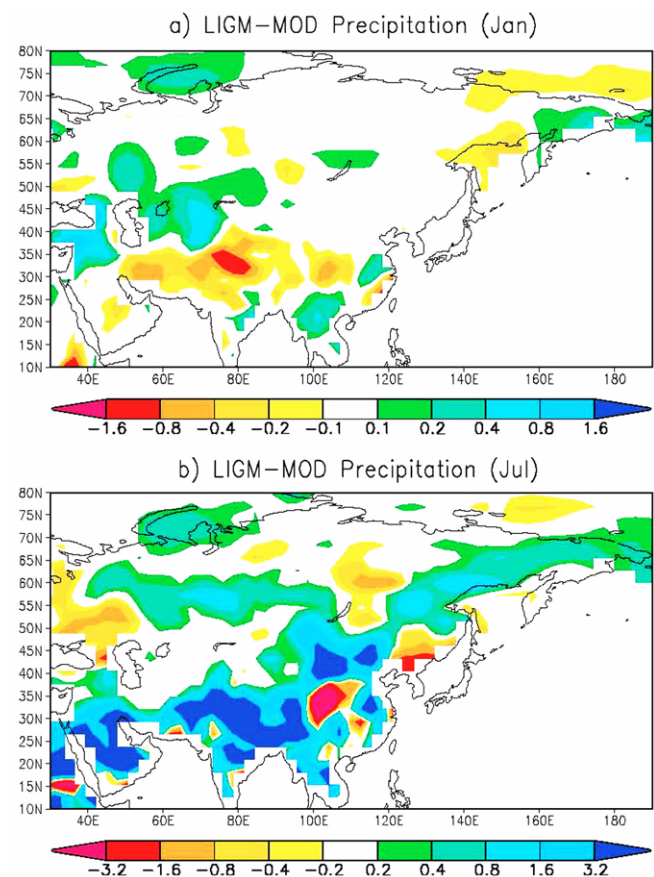


Fig. 11. Geographic distribution of the change in precipitation for a) January and b) July. Units are in mm day⁻¹.

suggested an increase in precipitation over Siberia and the northeast of Eurasia in winter, but the simulation shows a very little change in those areas.

In July, the precipitation increases in the latitude belt between 50° and 60°N, whereas there is little change to the north and south of this belt. This feature is consistent with proxy reconstructions. Velichko et al. (2007) suggested that in the LIGM summer the precipitation markedly increased in latitudes between 52° and 57°N, while it gradually decreases to the north and south of this latitude belt. They also suggested that in the eastern European Plain and in west Siberia, summer precipitation during the LIGM was close to the present-day level, while in Siberia and far east of the continent precipitation was greater than present. These observed features are well reproduced in the simulation, except over Siberia where the precipitation change in the simulation is very little or even slightly reduced in the LIGM.

In low to middle latitudes such as Saudi Arabia, northern India, south Asia, and north-eastern Asia, the simulated July precipitation increases substantially. The increase in precipitation over Saudi Arabia and northern India was also obtained in previous LIGM simulations. For example, using

LMD AGCM, De Noblet et al. (1996) obtained the precipitation increase over those regions by more than 5 mm/day, which is a similar amount obtained in this study. Using ECHAM/LSG coupled model and CLIMBER-2 intermediate complexity model, Kubatzki et al. (2000) obtained an increase in precipitation over northern India up to Saudi Arabia by 1–2 mm/day which is lower than the precipitation increase obtained in this study. Even though the southwest summer monsoon is simulated to be enhanced over Asia in the LIGM, in regions such as western China and north of Korea, precipitation appears to decrease. The reduction of precipitation in western China is at odds with paleoclimate proxy reconstructions because some paleosol and loess records showed an increase in rainfall during the LIGM (An et al., 1991; Heller et al., 1993; Liu et al., 1995; Wu et al., 2002; Jiang and Ding, 2005). Note, however, that proxy records representing rainfall in low to mid latitudes of Asia are limited and their uncertainties are relatively high.

3.3.6. Water transport

The distribution of precipitation is closely linked to the spatial wind pattern, which carries moisture from a place to

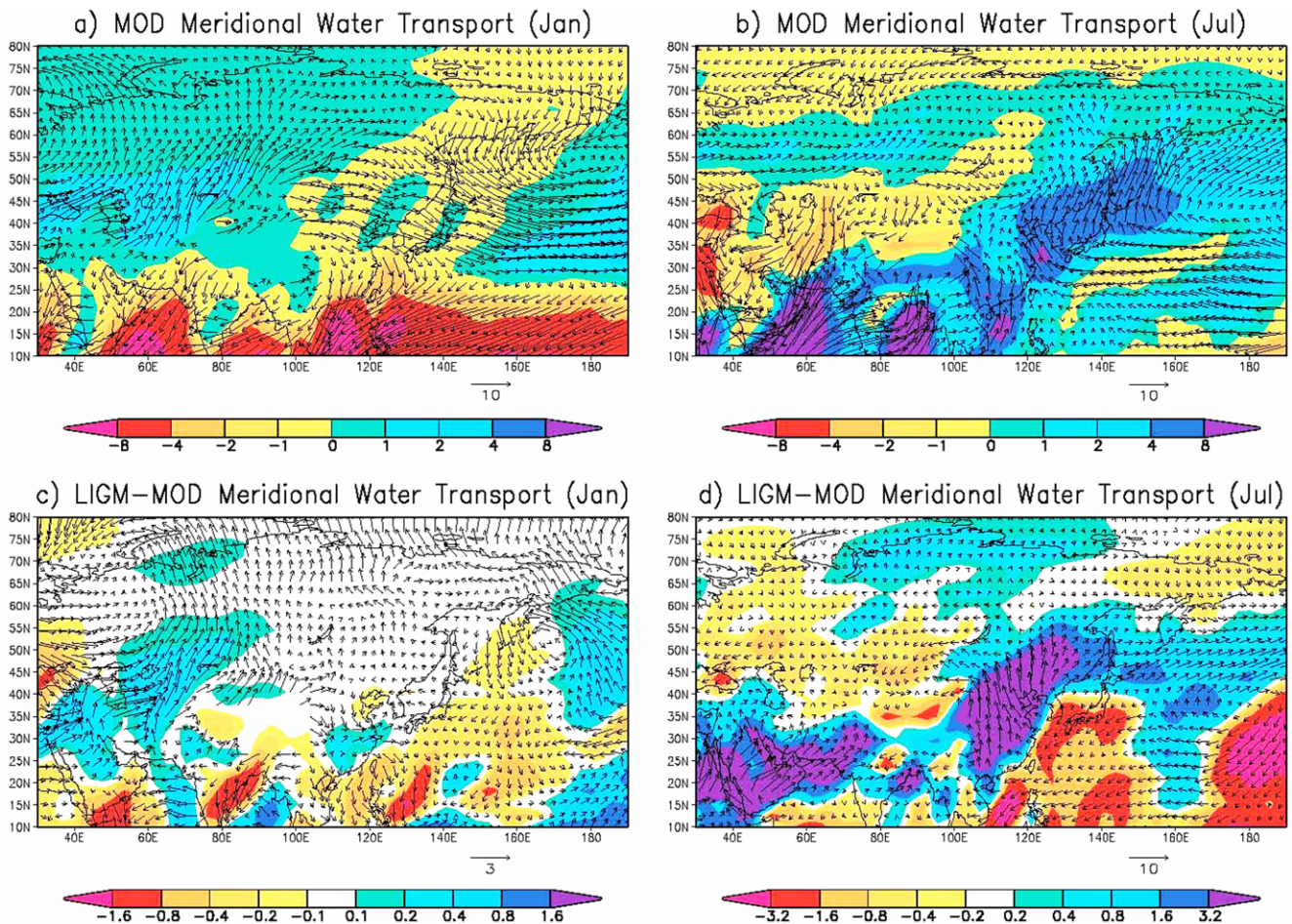


Fig. 12. Geographic distribution of the water transport simulated in the MOD for a) January and b) July, the change from the LIGM for c) January and d) July. Units are in cm s⁻¹ for water transport and m s⁻¹ for winds.

another. Figure 12 shows the January and July mean meridional water transport and their changes with wind vectors. In January, the northeast winds in south Asia and northwest winds in East Asia lead to the reduction in moisture transport, while in northern Asia the southerly winds tend to bring moisture even though the amount is very little. In July, the southwest winds in southern Asia and southeast winds in East Asia transport lots of moisture to south Asia, while in Middle East Asia the northerly winds result in those areas quite dry.

In the LIGM January, water transport slightly increases in Middle East Asia associated with the stronger southerly winds, which is consistent with the increase in precipitation seen in Figure 11a. In eastern India and south-eastern Asia, moisture transport decreases due to the development of northerly winds. In July, the southwest winds over the Arabian Sea and south winds in East Asia become stronger and the huge increase in water transport is obtained. Consequently, precipitation substantially increases over most of west, south, and east Asia including the now arid Middle East part. In mid-latitudes of western Asia and eastern Siberia, on the other hand, moisture transport decreases in the LIGM July, resulting in the reduction of precipitation. Overall, precipitation substantially increases in the LIGM over most parts of Asia, especially in July, associated with the increase in southwest and south winds.

4. SUMMARY AND CONCLUSION

This study explores the climate response in Asia/Arctic to the imposition of LIGM orbital conditions. The simulations were performed with the NCAR CCM3 atmospheric general circulation model at a spectral truncation of T42, corresponding to a horizontal resolution of about 2.8 degree. It has 18 vertical layers and includes comprehensive land surface processes. In the LIGM experiment, orbital parameters were set to 126 kBP, while SST and sea ice were prescribed with the modern values provided from NCAR.

Figure 13 schematically summarizes the change in surface air temperature in the LIGM in response to the change in orbital parameters. With the LIGM orbital conditions, the earth receives more energy in summer and less in winter because the perihelion occurs in July instead of January as in the present. This strengthens the seasonality of the insolation in the LIGM compared to the present. The insolation is modified while reaching the surface through atmosphere by a change in clouds. In July, a substantial warming and a slight cooling in mid to high latitudes are obtained, in consistent with the proxy records. The warming in mid to high latitudes is due to the increase in the net short-wave radiative heat fluxes, whereas the slight cooling in low latitudes is due to the reduction in the short-wave radiative heat fluxes by the increase in cloud amount.

In January, the net short-wave radiative heat flux is reduced

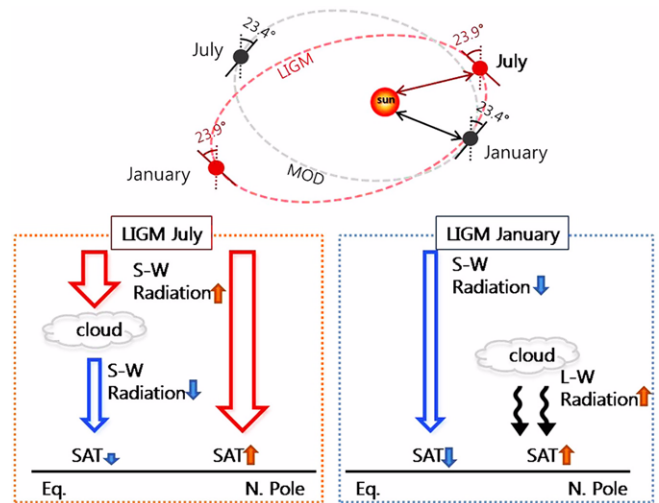


Fig. 13. Schematic diagram of the change in the earth's position, and radiative heat fluxes with clouds, and surface air temperature (SAT) in the LIGM compared to the MOD.

in low to mid latitudes and almost the same as present in high latitudes. The reduction in the net short-wave radiative heat fluxes lead to cooler conditions over low and mid latitudes of Asia and eastern Siberia. In northern Asia, a surface warming is simulated, in consistent with the proxy records, in spite of the little change in the short-wave radiative heat flux. Analysis indicates that the warming in northern Asia is due to the increase in the downward long wave heat fluxes associated with the increases in clouds. In January, the Arctic Oscillation (AO) polarity is enhanced in the LIGM, resulting in a slight warming over Siberia and part of the Arctic Ocean.

There is a little change in precipitation in January, whereas a substantial increase in precipitation is obtained in July over most Asia, especially the southern and middle eastern part. The increase in July precipitation is mainly due to the increase in southwest winds in the Indian Ocean and southerly winds over southeast Asia, indicating a stronger Asian monsoon in the LIGM as found in proxy reconstructions and previous model studies.

Overall, the orbital parameters for the LIGM lead to the surface temperature and precipitation in broadly consistent with those of proxy reconstructions. However, the degree of temperature and precipitation change in the simulation is substantially lower than those of reconstructions, especially in January accounting for less than 50% of the total surface climate change. Other conditions such as the ocean circulation and sea ice feedback must be included in illustrating the climate change over Asia/Arctic in the LIGM. In conclusion, the change in greenhouse effect associated with cloud feedback could play an important role in determining the climate change over Asia/Arctic under different climate background.

ACKNOWLEDGMENTS: We would like to acknowledge the support from KISTI (Korea Institute of Science and Technology Information) for using the computing system of the Supercomputing Center. Yoo-Min Park and Cho-Yeong Lee at Korea Polar Research Institute are especially appreciated for their help in preparing manuscript. This study was supported by Project of Integrated Research on the Composition of Polar Atmosphere and Climate Change (COMPAC) (PE10030) and Paleoclimate Modelling Study for Polar Regions (PE09120) of Korea Polar Research Institute. Sangheon Yi was supported by the Basic Research Project (GP2009-005) of the Korea Institute of Geoscience and Mineral Resources funded by the Ministry of Knowledge Economy of Korea.

REFERENCES

- Aalbersberg, G. and Litt, T., 1998, Multi-proxy climate reconstructions for the Eemian and Early Weichselian. *Journal of Quaternary Science*, 13, 367–390.
- Alekseev, M.N. and Golubeva, L.B., 1980, On the stratigraphy and paleogeography of the Late Pleistocene of the Southern Primoriye. *Bulleten Komissii po Izucheniyu Chetvertichnogo Perioda*, 50, 96–107.
- Andreev, A., Grosse, G., Schirrmeister, L., Kuzmina, S., Novenko, E., Bobrov, A., Tarasov, P., Ilyashuk, B., Kuznetsova, T., Krbetschek, M., Meyer, H., and Kunitsky, V., 2004, Late Saalian and Eemian palaeoenvironmental history of the Bol'shoy Lyakhovsky Island. Laptev Sea region, Arctic Siberia, *Boreas*, 33, 319–348.
- An, Z.S., Kukla, G., Porter, S.C., and Xiao, J.L., 1991, Magnetic susceptibility evidence of monsoon variation on the Loess Plateau of Central China during the last 130,000 years. *Quaternary Research*, 36, 29–36.
- Arslanov, K.A., Gei, N.A., Izmailov, Y.A., Lokshin, N.B., Gerasimova, S.A., and Tertychnyi, N.I., 1983, On the climatic conditions of formation and age of the deposits of the Late Pleistocene marine terraces on the shore of the Kerch Peninsula. *Vestnik Leningradskogo Universiteta*, 12, 69–79.
- Arkipov, S.A., Votakh, M.R., and Levina, T.P., 1973, Palynology of Riss–Würm (Kazantsevo) and Early–Middle Würm deposits in the middle Ob' River valley. In: Saks, V.N. (ed.), *Pleistotsen Sibiri i smezhnykh oblastei*, Nauka, Moscow, p. 143–150.
- Artyushenko, A.T., 1970, Forest–Steppe and Steppe Vegetation of Ukraine during the Quaternary. *Naukova Dumka*, Kiev, 174 p.
- Bloom, A.L., Broecker, W.S., Chappell, M.A., Matthews, R.K., and Mesolella, K.J., 1974, Quaternary sea-level fluctuations on a tectonic coast: New $^{230}\text{Th}/^{234}\text{U}$ dates from the Huon Peninsula. *New Guinea, Quaternary Research*, 4, 185–205.
- Boer, G.J., 1993, Climate change and the regulation of the surface moisture and energy budgets. *Climate Dynamics*, 8, 225–239.
- Bonan, G., 1998, The land surface climatology of the NCAR Land Surface Model coupled to the NCAR Community Climate Model. *Journal of Climate*, 11, 1307–1326.
- Boyarskaya, T.D., Sokhina, E.N., and Chernyuk, A.V., 1978, Results of the palynological studies of the Quaternary deposits in the lower Priamurye. In: Grichuk, M.P. and Korotkiy, A.M. (eds.), *Palinologicheskie Issledovaniya na Dal'nem Vostoke*, Far-East Scientific Center USSR Academy of Sciences, Vladivostok, p. 110–116.
- CAPE–Last Interglacial Project Members, 2006, Last Interglacial Arctic warmth confirms polar amplification of climate change. *Quaternary Research*, 25, 1383–1400.
- Chupina, L.N., 1978, Palynology of the Late Pleistocene deposits of the central and southern Kazakhstan. *Izvestiya Akademii Nauk Kazakhskoi SSR, Geological Series*, 3, 58–63.
- Cortijo, E., Duplessy, J.C., Labeyrie, L., Leclair, H., Duprat, J., and Van Weering, T.C.E., 1994, Eemian cooling in the Norwegian Sea and North Atlantic Ocean preceding continental ice-sheet growth. *Nature*, 372, 446–449.
- De Noblet, N., Braconnot, P., Joussaume, S., and Masson, V., 1996, Sensitivity of simulated Asian and African summer monsoons to orbitally induced variations in insolation 126, 115, 6 kBP. *Climate Dynamics*, 12, 589–603.
- De Vernal, A., Causse, C., Hillaire-Marcel, C., Mott, R.J., and Occhietti, S., 1986, Palynostratigraphy and Th/U ages of upper Pleistocene interglacial and interstadial deposits on Cape Breton Island, eastern Canada, *Geology*, 14, 554–557.
- Devyatova, E.I., 1982, Prirodnaya sreda pozdnego pleistotsena i yeyo vliyaniye na razvitiye cheloveka v Severodvinskom basseine I v Karelii (Late Pleistocene environments as related to human migrations in the Severnaya Dvina basin and in Karelia). *Petrozavodsk, Karelia*, 156 p.
- Devyatova, E.I. and Starova, N.N., 1970, Late Quaternary history of the Omega and Ladoga depressions as based on the palynological and diatom analyses. In: Basalikas, A.B. and Bagdonas, A.I. (eds.), *Istoriya Ozer*, Mintis, Vilnius, p. 82–100.
- Dodge, R.E., Fairbanks, R.G., Benninger, L.K., and Maurrasse, F., 1983, Pleistocene sea levels from raised coral reefs of Haiti. *Science*, 219, 1423–1425.
- EPICA Community members, 2006, One-to-one coupling of glacial climate variability in Greenland and Antarctica. *Nature*, 444, 195–198.
- Felis, T., Lohmann, G., Kuhnert, H., Lorenz, S.J., Scholz, D., Pätzold, J., Al-Rousan, S.A., and Al-Moghrabi, S.M., 2004, Increased seasonality in Middle East temperatures during the last interglacial period. *Nature*, 429, 164–168.
- Frenzel, B., Pecs, M., and Velichko, A., 1992, Atlas of Paleoclimates and Paleoenvironments of the Northern Hemisphere: Late Pleistocene–Holocene. Geographical Research Institute, Hungarian Academy of Sciences, Budapest; Gustav Fischer Verlag, Stuttgart, 153 p.
- Giterman, R.Y., 1963, Stages of development of the Quaternary vegetation in Yakutia and their stratigraphical importance. *Trudy Geologicheskogo Instituta AN SSSR*, 78, 1–192.
- Gong, D.Y., Wang, S.W., and Zhu, J.H., 2001, East Asian winter monsoon and Arctic Oscillation. *Geophysical Research Letters*, 28, 2073–2076.
- Gong, D.Y. and Ho, C.H., 2004, Intra-seasonal variability of wintertime temperature over East Asia. *International Journal of Climatology*, 24, 131–144.
- Gong, D.Y., Kim, S.J., and Ho, C.H., 2007, Arctic Oscillation and ice severity in the Bohai Sea. *East Asia, International Journal of Climatology*, 27, 1287–1302.
- Gorlova, R.N., 1967, Smena rastitel'nosti kak komponenta biogeotsenozov v predposlednee mezhdnednikov'e. *Nauka*, Moscow, 70 p.
- Granoszewski, W., Demske, D., Nita, M., Heumann, G., and Andreev, A.A., 2005, Vegetation and climate variability during the Last Interglacial evidenced in the pollen record from Lake Baikal. *Global and Planetary Change*, 46, 187–198.
- Grichuk, V.P., 1969, An experiment in reconstructing some characteristics in climate in the Northern hemisphere during the Atlanticum period of Holocene (in Russian). In: Neustadt, M. J. (ed.), *Holocene*, Akademia Nauk (Moscow), p. 41–57.
- Grichuk, V.P., Zelikson, E.M., and Nosov, A.A., 1983, New data on

- the interglacial deposits near Il'inskoye on the Yakhroma River. *Bulleten' Komissii po Izucheniyu Chetvertichnogo Perioda*, 52, 150–156.
- Grichuk, V.P., 1984, Late Pleistocene vegetation history. In: Velichko, A.A. (ed.), *Late Quaternary Environments of the Soviet Union*. University of Minnesota Press, Minneapolis, p. 155–178.
- Groll, N., Widmann, M., and Jones, J.M., 2005, Simulated relationships between regional temperature and large-scale circulation: 125 kyr BP (Emian) and the preindustrial period. *Journal of Climate*, 18, 4032–4045.
- Gudina, V.I., Kryukov, V.D., Levchuk, L.K., and Sudkov, L.A., 1983, Upper-Pleistocene sediments in northeastern Taimyr. *Bulletin of Commission on Quaternary Researches*, 52, 90–97 (in Russian).
- Gurtovaya, Y.Y., 1987, The climatic changes during the Mikulino-Kazantsevo Interglacial on the Russian Plain and in Siberia. *Izvestiya Akademii Nauk SSSR, Geographical Series*, 2, 54–62.
- Gurtovaya, Y.Y. and Faustova, M.A., 1977, On the Mikulino stage of the alluvium formation in the middle part of the Desna River basin (Posudichi section). *Izvestiya Akademii Nauk SSSR, Geographical Series*, 2, 69–75.
- Gurtovaya, Y.Y. and Krivonogov, S.K., 1988, Phytological characteristics of the Kazantsevo terrestrial deposits. In: Shatskiy, S.B. (ed.), *Mikrofosillii i Stratigrafiya Mezozoya i Kainzoya Sibiri*, SO Nauka, Novosibirsk, 69 p.
- Gurtovaya, Y.Y. and Troitskiy, S.L., 1968, On the palynology of the Sangamon deposits of the western Yamal. In: Saks, V.N. (eds.), *Neogenovye i Chetvertichnye Otlozheniya Zapadnoi Sibiri*. Nauka, Moscow, p. 131–140.
- Hall, A., Clement, A., Thompson, D.W.J., Broccoli, A.J., and Jackson, C., 2005, The Importance of Atmospheric Dynamics in the Northern Hemisphere Wintertime Climate Response to Changes in the Earth's Orbit. *Journal of Climate*, 18, 1315–1325.
- Harrison, S.P., Kutzbach, J.E., Prentice, I.C., Behling, P.J., and Sykes, M.T., 1995, The response of northern hemisphere extratropical climate and vegetation to orbitally induced changes in insolation during the Last Interglaciation. *Quaternary Research* 43, 174–184.
- Heller, F., Shen, C.D., Beer, J., Liu, X.M., Liu, T.S., Bronger, A., Suter, M., and Bonani, G., 1993, Quantitative estimates of pedogenic ferromagnetic mineral formation in Chinese loess and palaeoclimatic implications. *Earth and Planetary Science Letters*, 114, 385–390.
- Ivanova, N.G., 1973, Age estimation of the alluvial deposits of the Vyatka River and reconstruction of vegetation based on the palynological data. In: Grichuk, V.P. (ed.), *Palinologiya Pleistotsena i Plotsena*, Nauka, Moscow, p. 63–69.
- Jeong, J.H. and Ho, C.H., 2005, Changes in occurrence of cold surges over East Asia in association with Arctic Oscillation. *Geophysical Research Letters*, 32, L14704, doi: 10.1029/2005GL023024.
- Jiang, H. and Ding, Z., 2005, Temporal and spatial changes of vegetation cover on the Chinese Loess Plateau through the last glacial cycle: evidence from spore-pollen records. *Review of Palaeobotany and Palynology*, 133, 23–37.
- Joussau, S. and Braconnot, P., 1995, Sensitivity of Paleoclimate Simulation Results to Season Definitions. *Journal of Geophysical Research*, 102, 19431–19456.
- Keen, D.H., Harmon, R.S., and Andrews, J.T., 1981, U-series and amino acid dates from Jersey. *Nature*, 289, 162–164.
- Kaspar, F., Kühl, N., Cubasch, U., and Litt, T., 2005, A model-data-comparison of European temperatures in the Eemian interglacial. *Geophysical Research Letters*, 32, L11703, doi: 10.1029/2005GL022456.
- Kiehl, J.T., Hack, J.J., Bonan, B.G., Boville, B.A., Williamson, D.L., and Rasch, P., 1998a, The National Center for Atmospheric Research Community Climate Model: CCM3. *Journal of Climate*, 11, 1131–1149.
- Kiehl, J.T., Hack, J.J., and Hurrell, J., 1998b, The energy budget of the NCAR Community Climate Model: CCM3. *Journal of Climate*, 11, 1151–1178.
- Korotkiy, A.M., Karaulova, L.P., and Troitskaya, T.S., 1980, Quaternary deposits of Primor'e. *Stratigraphy and palaeogeography. Trudy Instituta Geologii i Gerfiziki SO AN SSSR*, 429, 233 p.
- Ku, T.L., Kimmel, M.A., Easton, W.H., and O'Neil, T.J., 1974, Eustatic sea level 120,000 years ago Oahu, Hawaii. *Science*, 183, 959–962.
- Kubatzki, C., Montoya, M., Rahmstorf, S., Ganopolski, S., and Clausen, M., 2000, Comparison of the last interglacial climate simulated by a coupled global model of intermediate complexity and an AOGCM. *Climate Dynamics*, 16, 799–814.
- Kukla, G.J., Bender, M.L., de Beaulieu, J.L., Bond, G., Broecker, W.S., Cleveringa, P., Gavin, J.E., Herbert, T.D., Imbrie, J., Jouzel, J., Keigwin, L.D., Knudsen, K.L., McManus, J.F., Merkt, J., Muhs, D.R., Müller, H., Poore, R.Z., Porter, S.C., Seret, G., Shackleton, N.J., Turner, C., Tzedakis, P.C., and Winograd, I.J., 2002, Last interglacial climates. *Quaternary Research*, 58, 2–13.
- LIGA Members, 1991, The last interglacial in high latitudes of the northern hemisphere: terrestrial and marine evidence. Report of the 1st discussion group. *Quaternary International*, 10–12, 9–28.
- Liu, X.M., Rolph, T., Bloemendal, J., Shaw, J., and Liu, T.S., 1995, Quantitative estimates of Palaeoprecipitation at Xifeng. in the Loess Plateau of China, *Palaeogeography, Palaeoclimatology, Palaeoecology*, 113, 243–248.
- Lozhkin, A.V. and Anderson, P.M., 1995, The last interglaciation in northeast Siberia. *Quaternary Research*, 43, 147–158.
- Lozhkin, A.V., Anderson, P.M., Matrosova, T.V., and Minyuk, P.S., 2007, The pollen record from El'gygytgyn Lake: implications for vegetation and climate histories of northern Chukotka since the late middle Pleistocene. *Journal of Paleolimnology*, 37, 135–153.
- Lu, J., Ju, J.-H., Kim, S.-J., Ren, J.-Z., and Zhu, Y.-X., 2008, The arctic oscillation and the autumn/winter snow depth over the Tibetan Plateau. *Journal of Geophysical Research*, 113, D14117, doi: 10.1029/2007JD009567.
- Lu, J., Kim, S.-J., Abe-Ouchi, A., Yu, Y., and Ohgaito, R., 2010, Arctic Oscillation during the mid-Holocene and the last glacial maximum from PMIP2 model simulations. *Journal of Climate* (in press).
- Malasova, E.S., 1989, Palynology of Novaya Zemlya. In: Kotlyakov, V.M. (ed.), *Moreny – Istochnik Glyatsiologicheskikh Dannyykh*. Nauka, Moscow, p. 182–200.
- Mamatsashvili, N.S., 1975, Palynological Characteristics of the Quaternary Terrestrial Deposits of Kolkhida. *Metsniereba, Tbilisi*, 114 p.
- Mangerud, J., Sonstegaard, E., Sejrup, H.P., and Haldorsen, S., 1981, Continuous Eemian-Early Weichselian sequence containing pollen and marine fossils at Fjosanger, western Norway. *Boreas*, 10, 137–208.
- Metel'tseva, E.P. and Sukachev, V.N., 1961, New data on the Pleistocene flora of the central Russian Plain (interglacial peat deposits from the Vladimir district). *Bulleten' Komissii po Izucheniyu Chetvertichnogo Perioda*, 26, 50–60.
- Miller, G.H., Sejrup, H.P., Mangerud, J., and Andersen, B.G., 1983, Amino acid ratios in Quaternary molluscs and foraminifera from western Norway: Correlation. geochronology and paleo-temperature estimates, *Boreas*, 12, 107–124.
- Montoya, M., Crowley, T.J., and von Storch, H., 1998, Temperatures at the last interglacial simulated by a coupled ocean-atmosphere

- climate model. *Paleoceanography*, 13, 170–177.
- Montoya, M., von Storch, H., and Crowley, T.J., 2000, Climate Simulation for 125 kyr BP with a Coupled Ocean–Atmosphere General Circulation Model. *Journal of Climate*, 13, 1057–1072.
- Muratova, M.V., 1973, The history of vegetation and climate development of the southeastern Chukotka during the Neogene and Pleistocene. Nauka, Moscow, 135 p.
- Nikol'skaya, M.V., 1980, Paleobotanical characteristics of the Late Pleistocene and Holocene deposits in Taimyr. In: Saks, V.N., Volkova, V.S., and Khlonova, A.F. (eds.), *Paleopalynologiya Sibiri*, Nauka, Moscow, p. 97–111.
- Nikonov, A.A. and Vostrukhina, T.M., 1964, On the stratigraphy of the Quaternary deposits of the north-eastern Kola Peninsula. *Doklady Akademii nauk SSSR*, 158, 104–107.
- Otto-Bliesner, B.L., Marshall, S.J., Overpeck, J.T., Miller, G.H., Hu, A., and CAPE Last Interglacial Project members, 2006, Simulating Arctic climate warmth and ice field retreat in the last interglaciation. *Science*, 311, 1751–1753.
- Peixoto, J.P. and Oort, A.H., 1992, *Physics of Climate*. Springer-Verlag, New York, AIP Press, 520 p.
- Petit, J.R., Jouzel, J., Raynaud, D., Barkov, N.I., Barnola, J.M., Basile, I., Bender, M., Chappellaz, J., Davis, M., Delaygue, G., Delmotte, M., Kotlyakov, V.M., Legrand, M., Lopenkov, V.Y., Lorius, C., Pepin, L., Ritz, C., Saltzman, E., and Stievenard, M., 1999, Climate and atmospheric history of the past 420,000 years from the Vostok ice core. *Antarctica. Nature*, 399, 429–436.
- Pleshivtseva, E.S., 1972, Palynology of the deposits of the Boreal transgression in the northwest of the Arkhangelsk district (Severnaya Dvina lowland). In: Grichuk, V.P. (ed.), *Palynologiya Pleistotsena*. Institut Geografii AN SSR, Moscow, p. 93–104.
- Prell, W.L. and Kutzbach, J.E., 1987, Monsoon variability over the past 150,000 years. *Journal of Geophysical Research*, 92, 8411–8425.
- Rindzjunskaia, N.M. and Pakhomov, M.M., 1977, On the stratigraphy of the Quaternary deposits of the Severo-Baikal'skie Mountains. *Izvestiya Akademii Nauk SSSR, Geological Series*, 4, 146–149.
- Rindzjunskaia, N.M., Reverdatto, M.V., Ivanov, N.M., Nedashkovskaya, N.N., and Zelikson, E.M., 1987, Characteristic features of Quaternary sedimentation in the Sub-Polar Urals, *Bulleten' Komissii po Izucheniyu Chetvertichnogo. Perioda*, 56, 111–118.
- Ruddiman, W.F. and Mckinstryre, A., 1976, Northeast Atlantic paleoclimatic changes over the past 600,000 years. In: Cline, R.M. and Hays, J.D. (eds.), *Investigation of Late Quaternary Paleoclimatology and Paleoclimatology*, Geological Society of America Memoirs, 145, p. 111–146.
- Skiba, L.A., 1975, The vegetation history of Kamchatka in the Late Pleistocene. *Trudy Geologicheskogo Instituta AN SSSR* 276, 208 p.
- Stuiver, M., Denton, G.H., Hughes, T.J., and Fastook, J.L., 1981, History of marine ice sheet in West Antarctica during the last glaciations: A working hypothesis. In: Denton, G.D. and Hughes, T.J. (eds.), *The Last Great Ice Sheets*. WileyInterscience, New York, p. 319–436.
- Suzuki, A., Gagan, M., De Deckker, P., Omura, A., Yukino, I., and Kawahata, H., 2001, Last Interglacial Coral Record of Enhanced Insolation Seasonality and Seawater ¹⁸O Enrichment in the Ryukyu Islands, Northwest Pacific. *Geophysical Research Letters*, 28, 3685–3688.
- Tarasov, P., Granoszewski, W., Bezrukova, E., Brewer, S., Nita, M., Abzaeva, A., and Oberhäsl, H., 2005, Quantitative reconstruction of the last interglacial vegetation and climate based on the pollen record from Lake Baikal, Russia. *Climate Dynamics*, 25, 625637.
- Thompson, D.W.J. and Wallace, J.M., 1998, The Arctic Oscillation signature in the wintertime geopotential height and temperature elds. *Geophysical Research Letters*, 25, 1297–1300.
- Thompson, D.W.J. and Wallace, J.M., 2000, Annular modes in the extratropical circulation part I: Month-to-month variability. *Journal of Climate*, 13, 1000–1016.
- Van der Hammen, T., Wijmstra, T.A., and Zagwijn, W.H., 1971, The floral record of the late Cenozoic of Europe. In: Turekian, K.K. (ed.), *The Late Cenozoic Glacial Ages*. Yale University Press, New Haven, Connecticut, p. 391–424.
- Velichko, A.A., Kremenetski, C.V., Borisova, O.K., Zelikson, E.M., Nechaev, V.P., and Faure, H., 1998, Estimate of methane emission during the last 125,000 years in Northern Eurasia. *Global and Planetary Change*, 16–17, 159–180.
- Velichko, A.A., Borisova, O.K., and Zelikson, E.M., 2007, Proxies of the Last Interglacial climate: reconstruction of northern Eurasia climate based on paleofloristic data. *Boreas*, 37, doi: 10.1111/j.1502-3885.2007.
- Volkova, V.S., Gurtovaya, Y.Y., and Levchuk, L.K., 1988, Palynology of the marine deposits of the Kazantsevo horizon in the lower Yenisei basin. In: Shatskiy, S.B. (ed.), *Mikrofosillii i stratigrafiya Mezozoyz i Kainozoya Sibiri*, SO Nauka, Novosibirsk, p. 31–41.
- Wolard, G.M., 1978, Grande Pile peat bog: A continuous pollen record for the last 140,000 years. *Quaternary Research*, 9, 1–21.
- Wu, B.Y. and Wang, J., 2002, Winter Arctic Oscillation, Siberian High and East Asian winter monsoon. *Geophysical Research Letters*, 29, 197, doi: 10.1029/2002GL015373.
- Wu, G., Pan, B., Guan, Q., Liu, Z., and Li, J., 2002, Loess record of climatic changes during MIS5 in the Hexi Corridor, northwest China. *Quaternary international*, 97–98, 167–172.
- Yuan, D., Cheng, H., Lawrence Edwards, R., Dykoski, C.A., Kelly, M.J., Zhang, M., Qing, J., Lin, Y., Wang, Y., Wu, J., Dorale, J.A., An, Z., and Cai, Y., 2004, Timing, Duration, and Transitions of the Last Interglacial Asian Monsoon. *Science*, 304, 575–578.
- Zagwijn, W.H., 1996, An analysis of Eemian climate in Western and Central Europe. *Quaternary Science Reviews*, 15, 451–469.

Manuscript received March 30, 2009

Manuscript accepted April 6, 2010